

# Trajectory-Oriented Policy Optimization with Sparse Rewards

1<sup>st</sup> Guojian Wang

*School of Mathematical Sciences*  
*Beihang University*  
Beijing, China  
wgj@buaa.edu.cn

2<sup>nd</sup> Faguo Wu\*

*Institute of Artificial Intelligence*  
*Beihang University*  
Beijing, China  
faguo@buaa.edu.cn

3<sup>rd</sup> Xiao Zhang

*School of Mathematical Sciences*  
*Beihang University*  
Beijing, China  
xiao.zh@buaa.edu.cn

\*Corresponding author

\*Corresponding author

**Abstract**—Mastering deep reinforcement learning (DRL) proves challenging in tasks featuring scant rewards. These limited rewards merely signify whether the task is partially or entirely accomplished, necessitating various exploration actions before the agent garners meaningful feedback. Consequently, the majority of existing DRL exploration algorithms struggle to acquire practical policies within a reasonable timeframe. To address this challenge, we introduce an approach leveraging offline demonstration trajectories for swifter and more efficient online RL in environments with sparse rewards. Our pivotal insight involves treating offline demonstration trajectories as guidance, rather than mere imitation, allowing our method to learn a policy whose distribution of state-action visitation marginally matches that of offline demonstrations. We specifically introduce a novel trajectory distance relying on maximum mean discrepancy (MMD) and cast policy optimization as a distance-constrained optimization problem. We then illustrate that this optimization problem can be streamlined into a policy-gradient algorithm, integrating rewards shaped by insights from offline demonstrations. The proposed algorithm undergoes evaluation across extensive discrete and continuous control tasks with sparse and misleading rewards. The experimental findings demonstrate the significant superiority of our proposed algorithm over baseline methods concerning diverse exploration and the acquisition of an optimal policy.

**Index Terms**—deep reinforcement learning, sparse rewards, efficient exploration, offline demonstrations

## I. INTRODUCTION

Reinforcement learning (RL) has showcased remarkable efficacy in addressing intricate decision-making challenges through iterative learning [1]–[3]. Nevertheless, when confronted with sparse or delayed environmental reward signals, these RL methodologies may encounter inefficiencies in sample complexity and suboptimal performance. This primarily stems from the inherent challenge of navigating environments effectively and the limited availability of immediate reward cues [4], [5]. Additionally, real-world tasks often feature ambiguously defined objectives, making it challenging to devise precise reward functions for these endeavors [6]. Consequently, this practical dilemma imposes demanding criteria on DRL techniques to be viable within sparse reward scenarios.

This work was supported by the National Key R&D Program of China (2022ZD0116401), Fundamental Research Funds for the Central Universities, and the National Natural Science Foundation of China(Grant Nos. 62141605).

Addressing this limitation not only enhances the applicability of DRL to real-world scenarios but also significantly broadens the potential impact of RL methodologies.

Reward engineering is an alternative and direct way to provide dense and significant reward signals, which mainly refers to manually designing reward function [7], [8]. Unfortunately, building a specified reward function may require extensive instrumentation, such as thermal cameras to detect liquids pouring [9], and accelerometers to detect door opening [10]. Moreover, it may still be hard to construct a handcrafted and suitable reward function because of undue reward exploitation. Specifically, RL agents often discover unexpected and unintended ways to fulfill high returns and cater to biased objective functions [7].

Another promising approach to conquering the sparse-reward difficulty is learning from demonstrations (LfD). LfD methods leverage offline expert demonstrations to enhance the performance of DRL algorithms [11]–[13]. Some LfD methods only regard demonstrations as data augmentations without fully utilizing them in the policy optimization process [14]. Many other studies accelerate policy optimization by pre-training the policy with demonstrations in a supervised manner [3]. Furthermore, recent LfD research proposes encouraging the agent to mimic the expert action distribution, which takes inspiration from imitation learning (IL). However, these methods often require offline demonstrations to be perfect and sufficient, burdening human experts more [15].

This study develops a simple and feasible reinforcement learning method, called **Trajectory Oriented Policy Optimization** (TOPO), which can encourage efficient exploration in tasks with sparse rewards. TOPO avoids introducing complicated models or prior knowledge to obtain a reliable and feasible reward function. Meanwhile, TOPO overcomes the drawbacks of RLfD methods and reduces the RLfD's demonstration quantity requirement. Our crucial insight lies in acknowledging offline demonstration trajectories as guidance, rather than mimicking them. TOPO incentivizes the agent to acquire a policy whose distribution of state-action visitation marginally aligns with that of offline demonstrations. In particular, we introduce a unique trajectory distance founded on maximum mean discrepancy (MMD), and we frame policy

optimization as a distance-constrained optimization problem. Subsequently, we illustrate that this optimization problem can be streamlined into a policy-gradient algorithm incorporating rewards shaped by insights gleaned from offline demonstrations. The proposed algorithm undergoes evaluation across extensive discrete and continuous control tasks characterized by sparse and misleading rewards. Substantial experimental findings conclusively demonstrate that TOPO outperforms other baseline algorithms in diverse environments with sparse rewards.

## II. PRELIMINARIES

### A. Reinforcement Learning

A standard RL issue can be characterized as a discrete-time Markov decision process (MDP). This paper employs a tuple  $M = (\mathcal{S}, \mathcal{A}, P, r, \rho_0, \gamma)$  to represent a Markov decision process. In this context,  $\mathcal{S}$  signifies either a discrete or continuous state space, while  $\mathcal{A}$  represents a discrete (or continuous) action space. The function  $P : \mathcal{S} \times \mathcal{A} \rightarrow \Pi(\mathcal{S})$  denotes a transition probability distribution, where  $\Pi(\mathcal{S})$  indicates the space of probability distributions over a state  $\mathcal{S}$ . Furthermore,  $r_e : \mathcal{S} \times \mathcal{A} \rightarrow [R_{\min}, R_{\max}]$  characterizes the reward function, where  $R_{\min}$  and  $R_{\max}$  define the minimum and maximum values of the reward function  $r_e$ , respectively. Meanwhile,  $\rho_0$  represents the initial state distribution, and  $\gamma \in [0, 1]$  serves as a discount factor. The policy  $\pi_\theta : \mathcal{S} \rightarrow \mathcal{P}(\mathcal{A})$  is parameterized by  $\theta$  and maps the state space  $\mathcal{S}$  to a collection of action probability distributions over the action space  $\mathcal{A}$ . Typically, the RL objective function aims to maximize the expected discounted return as follows:

$$J(\pi_\theta) = \mathbb{E}_{s_0, a_0, \dots} \left[ \sum_{t=0}^{\infty} \gamma^t r_e(s_t, a_t) \right]. \quad (1)$$

In the above equation,  $s_0$  is sampled from  $\rho_0(s_0)$ ,  $a_t$  is drawn from  $\pi_\theta(a_t|s_t)$ , and  $s_{t+1}$  is sampled from  $P(s_{t+1}|s_t, a_t)$ . Additionally, this article adheres to the conventional definitions of the state-action value function  $Q_\pi$  and the value function  $V_\pi$ :

$$Q_\pi(s_t, a_t) = \mathbb{E}_{s_{t+1}, a_{t+1}} \left[ \sum_l \gamma^l r_e(s_{t+l}, a_{t+l}) \right], \quad (2)$$

and

$$V_\pi(s_t) = \mathbb{E}_{a_t, s_{t+1}, a_{t+1}} \left[ \sum_l \gamma^l r_e(s_{t+l}, a_{t+l}) \right], \quad (3)$$

In this scenario,  $s_0$  is sampled following  $\rho_0(s_0)$ ,  $a_t$  is drawn from  $\pi_\theta(a_t|s_t)$ , and  $s_{t+1}$  is sampled according to  $P(s_{t+1}|s_t, a_t)$ . Subsequently, the advantage function is expressed as:

$$A_\pi(s_t, a_t) = Q_\pi(s_t, a_t) - V_\pi(s_t). \quad (4)$$

For  $\gamma < 1$ , the discounted distribution of state visitation  $d_\pi$  is formulated as follows:  $d_\pi(s) = (1 - \gamma) \sum_{t=0}^{\infty} \gamma^t \mathbb{P}(s_t = s | \pi)$ , where  $\mathbb{P}(s_t = s | \pi)$  represents the probability of  $s_t = s$  considering the randomness introduced by  $\pi$ ,  $P$ , and  $\rho_0$ .

### B. Maximum Mean Discrepancy

Maximum Mean Discrepancy (MMD) stands as a crucial probability metric, gauging the distinction between any two probability distributions [16], [17]. Consider  $p$  and  $q$  as probability distributions specified within a nonempty compact metric space  $\mathbb{X}$ . Let  $x$  and  $y$  denote observations independently sampled from  $p$  and  $q$ , respectively. Following this, the MMD metric between  $p$  and  $q$  is precisely defined as

Suppose  $\mathcal{F}$  represents the Reproducing Kernel Hilbert Space (RKHS)  $\mathcal{H}$  featuring a kernel function  $k \in \mathcal{H}$ , like the Gaussian or Laplace kernel functions. The MMD metric between  $p$  and  $q$  is subsequently defined, as indicated by [17], [18].

$$\text{MMD}^2(p, q, \mathcal{H}) = \mathbb{E}[k(x, x')] - 2\mathbb{E}[k(x, y)] + \mathbb{E}[k(y, y')], \quad (5)$$

where  $x, x'$  i.i.d.  $\sim p$  and  $y, y'$  i.i.d.  $\sim q$ .

## III. PROPOSED APPROACH

This section presents a strategy for exploration guided by trajectories in DRL. This addresses the challenge of hard exploration in DRL through the lens of constrained optimization. Our fundamental idea is to prompt an RL agent to systematically explore the portion of the state space corresponding to the extension of demonstration trajectories.

### A. Trajectory-Guided Exploration Strategy

We suggest reformulating a unique constrained optimization problem to promote effective exploration in environments with sparse rewards. Assume a set  $\mathcal{M}$  comprises offline demonstration trajectories leading to imperfect sparse rewards, indicating these demonstrations may not be generated by the optimal policy. Our objective is to guide the agent to explore the targeted region of the state space alongside these demonstration trajectories, avoiding unnecessary exploration. One approach to realizing this objective is to minimize the distinction between the current and demonstration trajectories. Specifically, we employ the squared MMD metric, as defined in (5), to quantify the difference between diverse trajectories.

In each iteration of the training process, the agent generates multiple trajectories based on  $\pi$  and archives them in the on-policy trajectory buffer  $\mathcal{B}$ . Each trajectory  $\tau$  present in the buffer  $\mathcal{B}$  and the offline demonstration dataset  $\mathcal{M}$  is regarded as a deterministic policy. Subsequently, we compute its state-action visitation distribution  $\rho_\tau$ . The squared MMD distance is then computed between the state-action visitation distributions of the offline demonstration trajectory in  $\mathcal{M}$  and the current trajectory in  $\mathcal{B}$ . To be precise, following (5), the squared MMD distance between the distributions of state-action within trajectories is expressed as:

$$\begin{aligned} \text{MMD}^2(\tau, v, \mathcal{H}) = & \mathbb{E}_{x, x' \sim \rho_\tau} [k(x, x')] \\ & - 2 \mathbb{E}_{\substack{x \sim \rho_\tau \\ y \sim \rho_v}} [k(x, y)] \\ & + \mathbb{E}_{y, y' \sim \rho_v} [k(y, y')]. \end{aligned} \quad (6)$$

In this context,  $\tau$  belongs to  $\mathcal{B}$ ,  $v$  belongs to  $\mathcal{M}$ , and  $x, x', y, y'$  represent pairs of state and action. The state-action visitation

distributions of  $\tau$  and  $v$  are denoted as  $\rho_\tau$  and  $\rho_v$ , respectively. The function  $k(\cdot, \cdot)$  is defined as:

$$k(x, y) = K(g(x), g(y)). \quad (7)$$

In this context,  $K(\cdot, \cdot)$  represents the kernel of a reproducing kernel Hilbert space  $\mathcal{H}$ , such as a Gaussian kernel.

The function  $g$  in (7) allows for flexible adjustment of the focus in the squared MMD distance concerning various aspects, such as state visits, action choices, or both. This investigation exclusively computes the MMD distance related to an information subset within each state-action pair. Specifically, this subset is determined as the coordinate  $c$  of the center of mass (CoM), implying that the function  $g$  maps a state-action pair  $(s, a)$  to  $c$ . Additionally, multiple options exist for the function  $g$ . For instance, it might be reasonable to let  $g(s, a) = (c, a)$ , although this could entail the design of a new kernel function  $K(\cdot, \cdot)$ . Ultimately, we introduce a novel metric  $D(x, \mathcal{M})$  to assess the distance between the state-action pair  $x = (s, a)$  in  $\mathcal{B}$  and the offline demonstration dataset  $\mathcal{M}$  as follows:

$$D(x, \mathcal{M}) = \mathbb{E}_{\tau \in \mathcal{B}_x} [\text{MMD}^2(\tau, \mathcal{M}, \mathcal{H})]. \quad (8)$$

In this context,  $\mathcal{B}_x = \{\tau | x \in \tau, \tau \in \mathcal{B}\}$ , and the squared  $\text{MMD}^2(\tau, \mathcal{M}, \mathcal{H})$  is delineated as:

$$\text{MMD}^2(\tau, \mathcal{M}, \mathcal{H}) = \min_{v \in \mathcal{M}} \text{MMD}^2(\tau, v, \mathcal{H}). \quad (9)$$

To underscore that the distance measurement in Eq. (8) relies on the maximum mean discrepancy, we introduce the subscript MMD to the symbol  $D$ . The stochastic optimization problem, incorporating constraints related to MMD distance, is outlined as follows:

$$\begin{aligned} & \max_{\theta} J(\theta), \\ & \text{s.t. } D_{\text{MMD}}(x, \mathcal{M}) \leq \delta, \quad \forall x \in \mathcal{B}. \end{aligned} \quad (10)$$

Here,  $J$  denotes a standard objective in reinforcement learning, while  $\delta$  stands for a constant boundary constraint on distance.

**Remark 1.** *The update of replay memory  $\mathcal{M}$  takes place during policy optimization. Should a current trajectory outperform trajectories within  $\mathcal{M}$ —for instance, exhibiting a higher return—it becomes feasible to substitute the trajectory with the lowest return in  $\mathcal{M}$  with the superior one. Additionally, the initial offline trajectories can be sourced from human players. The fundamental concept of our study revolves around aligning its policy in proximity to offline demonstrations by treating them as soft guidance. In contrast to RLfD methods, our approach doesn't necessitate flawless and ample demonstrations, presenting a more practical scenario.*

## B. Practical Algorithms

To address the optimization problem posed in (10), we convert it into an unconstrained objective function, yielding the subsequent expression:

$$L(\theta, \sigma) = J(\theta) - \sigma \mathbb{E}_{x \sim \rho_\pi} [\max \{D_{\text{MMD}}(x, \rho_\mu) - \delta, 0\}]. \quad (11)$$

Here, the Lagrange multiplier  $\sigma$  is a positive value.

Following this, we compute the policy gradient for the unconstrained optimization problem. The initial component of the unconstrained problem represents the standard RL objective function, and as a result, obtaining its gradient is straightforward [19]. Subsequently, we deduce the gradient for the MMD term in (11), facilitating the efficient optimization of the policy. The outcome is articulated in the ensuing lemma.

**Lemma 1** (Gradient Derivation of the MMD term). *Consider  $\rho_\pi(s, a)$  as the state-action visitation distribution generated by the existing policy  $\pi$ . Define  $D(x, \mathcal{M})$  as the MMD distance between the state-action pair  $x$  and the offline demonstration buffer  $\mathcal{M}$ . If the policy  $\pi$  is characterized by parameters  $\theta$ , the gradient of the MMD term in (11) with respect to the parameters  $\theta$  is derived as follows:*

$$\nabla_\theta D_{\text{MMD}} = \mathbb{E}_{\rho_\pi(s, a)} [\nabla_\theta \log \pi_\theta(a|s) Q_i(s, a)], \quad (12)$$

where

$$Q_i(s_t, a_t) = \mathbb{E}_{\rho_\pi(s, a)} \left[ \sum_{l=0}^{T-t} \gamma^l R_i(s, a) \right], \quad (13)$$

and

$$R_i(s, a) = \max \{D_{\text{MMD}}(x, \mathcal{M}) - \delta, 0\}. \quad (14)$$

*Proof.* Consider  $x$  as the representation for a state-action pair, where  $x = (s, a)$ . Define  $R_i(s, a)$  as the intrinsic reward function obtained from the maximum mean discrepancy:

$$R_i(s, a) = \max \{D_{\text{MMD}}(x, \mathcal{M}) - \delta, 0\}.$$

Furthermore, let  $Q_i(\cdot, \cdot)$  represent the  $Q$ -function computed using  $R_i(s, a)$  as the reward:

$$Q_i(s_t, a_t) = \mathbb{E} \left[ \sum_{l=0}^{T-t} \gamma^l R_i(s_{t+l}, a_{t+l}) \right].$$

The gradient of (11) can be readily computed using the policy gradient theorem [20].

$$\nabla_\theta D_{\text{MMD}} = \mathbb{E}_{\rho_\pi(s, a)} [\nabla_\theta \log \pi_\theta(a|s) Q_i(s, a)].$$

For simplicity, we omit the specific derivation process.  $\square$

## IV. EXPERIMENTS

In this section, for a comprehensive evaluation of the TOPO algorithm, we subjected it to testing in three distinct environments featuring both discrete and continuous action spaces, as detailed in Section IV-A. The outcomes of our experiments illustrate that TOPO surpasses alternative baseline methods in terms of both learning rate and average return.

---

**Algorithm 1:** TOPO based on PPO

---

**Input:** learning rate  $\alpha$ , offline demonstration dataset  $\mathcal{M}$ , policy update frequency  $K$

- 1: Initialize policy weights  $\theta$  of each agent.
- 2: // BUFFER THAT STORES OFFLINE DEMONSTRATION TRAJECTORIES
- 3: Initialize  $\mathcal{M} \leftarrow \{\tau_{demo}\}$
- 4: **for** episode  $\in \{0, \dots, T\}$  **do**
- 5:    $\tau \leftarrow \emptyset$  // STORE STATE-ACTION PAIRS
- 6:    $R \leftarrow 0$  // ACCUMULATE REWARDS
- 7:   **for** each step in  $\{1, \dots, T\}$  **do**
- 8:     Choose  $a$  from  $s$  using  $\pi_\theta$
- 9:     take action  $a$  and observe  $r_e$  and  $s'$
- 10:     $\tau \leftarrow \tau \cup \{(s, a)\}; R \leftarrow R + r_e$
- 11:   **end for**
- 12:   Compute the MMD distance  $D_{\text{MMD}}(x, \mathcal{M})$  for each state-action pair  $x$  of this episode
- 13:   **if** episode  $\% K == 0$  **then**
- 14:     Estimate the MMD gradient  $\nabla_\theta D_{\text{MMD}}$  using  $\mathcal{M}$  and  $\mathcal{B}$
- 15:     Estimate the policy gradient  $\nabla_\theta J$  based on  $\mathcal{B}$
- 16:     Calculate the final gradient
- 17:      $\nabla_\theta L = \nabla_\theta J - \sigma \nabla_\theta D_{\text{MMD}}$
- 18:     // UPDATE THE POLICY PARAMETER
- 19:      $\theta \leftarrow \theta + \alpha \nabla_\theta L$
- 20:   **end if**
- end for**

---

#### A. Experimental Settings

The initial assessment of TOPO’s performance was conducted in the Key-Door-Treasure task, as illustrated in Fig. 1. This task’s state-action space is discrete, and the grid-world maze dimensions are  $26 \times 36$ . In each episode, the agent commences from a fixed starting point in the bottom-left room. The episode’s duration is fixed, terminating immediately upon the agent discovering the treasure. A positive reward of 200 is exclusively granted when the treasure is reached, and no rewards are provided in other instances. At each time step, the agent observes its environmental position and selects an action based on its prevailing policy: *move east, west, south, or north*. To locate the treasure, the agent must acquire the key (K) to unlock the door (D) and then traverse the room in the upright corner to access the treasure (T). TOPO’s performance was benchmarked against four baseline methods: PPO [19], SIL [11], PPO+D [14], and Noisy-A2C [21].

As depicted in Figs. 2a and 2b, we showcased TOPO’s dominance in two sparse MuJoCo locomotion tasks featuring continuous state-action spaces. To explore the potential benefits of TOPO in more formidable learning endeavors, we adapted two established MuJoCo agents, HalfCheetah and Hopper, yielding two novel agents denoted as SparseHalfCheetah and SparseHopper. These agents exclusively receive rewards based on forward velocity when the centers of the robots’ mass have advanced toward a specific direction beyond a predetermined

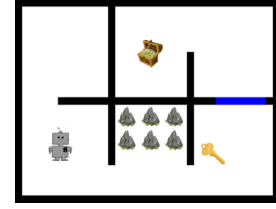


Fig. 1. Key-Door-Treasure domain.

threshold distance; otherwise, no positive rewards are accrued. The threshold distance is set at 1 unit for SparseHopper and 10 units for SparseCheetah. At each time step, the agent observes environmental cues and executes an action sampled from the policy. Additionally, an energy penalty is incurred by the agent’s movement, influencing the torque applied to the robot joints. TOPO’s performance was juxtaposed against three baseline methods: PPO [19], PPO+D [14], and GASIL [22].

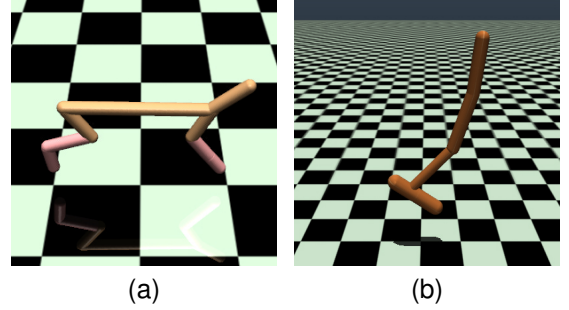


Fig. 2. (a) SparseHalfCheetah; (b) SparseHopper.

#### B. Results in the Key-Door-Treasure domain

Illustrated in Fig. 1, within the key-door-treasure scenario, securing the ultimate treasure mandates the agent’s sequential completion of three distinct tasks: procuring the key, unlocking the door, and ultimately acquiring the treasure. It is noteworthy that, for equitable evaluation, we endowed the SIL agent with identical demonstration data to that of TOPO at the initiation of policy optimization. The PPO agent, often entangled in a sub-optimal policy solely focused on key acquisition, fails to achieve optimal rewards upon reaching the treasure. Noisy-A2C exhibits analogous training outcomes to PPO. In contrast, the robust baselines, SIL and PPO+D, demonstrate accelerated learning facilitated by the exploration bonus derived from the demonstration data, leading them to discover the treasure. Notably, TOPO attains competitive training performance comparable to PPO+D, surpassing SIL in this task. This outcome signifies TOPO’s adeptness in efficient exploration of environments by leveraging demonstration trajectories to redefine a constrained optimization problem.

#### C. Comparisons on locomotion control tasks

Displayed in Figs. 4a and 4b, TOPO exhibits superior performance compared to other baseline methods in the SparseHopper and SparseCheetah tasks. Specifically, TOPO

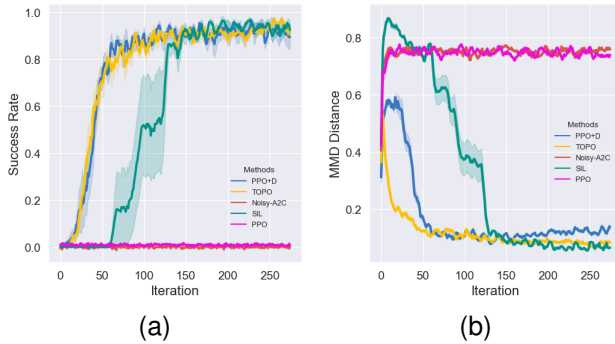


Fig. 3. (a) Success rate in the Key-Door-Treasure domain; (b) The changing trend of the MMD distance;

demonstrates accelerated learning during policy optimization, attaining a higher final return after training. GASIL focuses solely on discerning disparities between the state-action visitation distributions of the current policy and sparse-reward demonstration data, constructing a reward function based on this discrepancy. However, this approach places a premium on sample quality, limiting its competitiveness against TOPO. PPO+D relies exclusively on the advantage information from demonstrations for policy gradient computation, resulting in inefficient policy optimization with offline demonstrations. This discrepancy in approach contributes to the performance gap between PPO+D and TOPO. Noteworthy is the stagnation in the average return of PPO+D on the SparseHopper task throughout training, underscoring TOPO's efficacy in exploration by incorporating distribution information from sparse-reward demonstrations and defining a dense reward function based on the MMD distance.

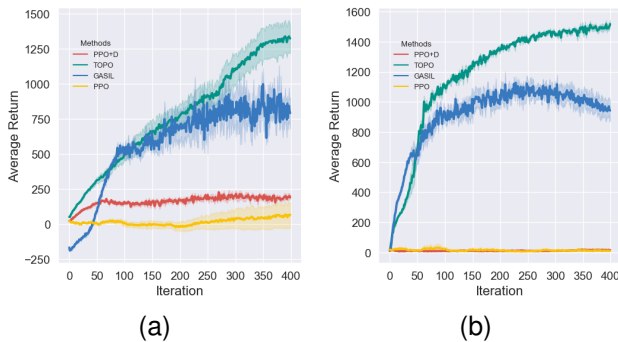


Fig. 4. (a) Learning curves of average return on the SparseHalfCheetah task; (b) Learning curves of average return on the SparseHopper task.

## V. CONCLUSIONS

This study presents TOPO, an approach designed to expedite and enhance online Reinforcement Learning (RL) using offline demonstrations in tasks characterized by sparse rewards. TOPO sidesteps the need for intricate reward function models, minimizing the reliance on a large number of demonstrations. The central concept involves training a

policy aligning its state-action visitation distribution with offline demonstrations, treating these trajectories as instructive guides. Specifically, we introduce a novel trajectory distance metric based on Maximum Mean Discrepancy (MMD) and cast policy optimization as a distance-constrained optimization challenge. Consequently, we demonstrate that this distance-constrained optimization problem can be transformed into a policy-gradient algorithm incorporating shaped rewards acquired from offline demonstrations. The proposed algorithm is extensively evaluated across discrete and continuous control tasks, featuring sparse and deceptive rewards. The experimental outcomes underscore TOPO's superiority over baseline methods in terms of diverse exploration and the ability to circumvent local optima.

## REFERENCES

- [1] V. Mnih, K. Kavukcuoglu, D. Silver, A. A. Rusu, J. Veness, M. G. Bellemare, A. Graves, M. Riedmiller, A. K. Fidjeland, G. Ostrovski *et al.*, “Human-level control through deep reinforcement learning,” *nature*, vol. 518, no. 7540, pp. 529–533, 2015.
- [2] V. Mnih, A. P. Badia, M. Mirza, A. Graves, T. Lillicrap, T. Harley, D. Silver, and K. Kavukcuoglu, “Asynchronous methods for deep reinforcement learning,” in *International conference on machine learning*. PMLR, 2016, pp. 1928–1937.
- [3] D. Silver, A. Huang, C. J. Maddison, A. Guez, L. Sifre, G. Van Den Driessche, J. Schrittwieser, I. Antonoglou, V. Panneershelvam, M. Lanctot *et al.*, “Mastering the game of go with deep neural networks and tree search,” *nature*, vol. 529, no. 7587, pp. 484–489, 2016.
- [4] T. Yang, H. Tang, C. Bai, J. Liu, J. Hao, Z. Meng, P. Liu, and Z. Wang, “Exploration in deep reinforcement learning: a comprehensive survey,” *arXiv preprint arXiv:2109.06668*, 2021.
- [5] G. Wang, F. Wu, X. Zhang, N. Guo, and Z. Zheng, “Adaptive trajectory-constrained exploration strategy for deep reinforcement learning,” *Knowledge-Based Systems*, p. 111334, 2023.
- [6] H. J. Jeon, S. Milli, and A. Dragan, “Reward-rational (implicit) choice: A unifying formalism for reward learning,” *Advances in Neural Information Processing Systems*, vol. 33, pp. 4415–4426, 2020.
- [7] A. M. Turner, D. Hadfield-Menell, and P. Tadepalli, “Conservative agency via attainable utility preservation,” in *Proceedings of the AAAI/ACM Conference on AI, Ethics, and Society*, 2020, pp. 385–391.
- [8] T. R. Sumers, M. K. Ho, R. D. Hawkins, K. Narasimhan, and T. L. Griffiths, “Learning rewards from linguistic feedback,” in *Proceedings of the AAAI Conference on Artificial Intelligence*, vol. 35, no. 7, 2021, pp. 6002–6010.
- [9] C. Schenck and D. Fox, “Visual closed-loop control for pouring liquids,” in *2017 IEEE International Conference on Robotics and Automation (ICRA)*. IEEE, 2017, pp. 2629–2636.
- [10] A. Yahya, A. Li, M. Kalakrishnan, Y. Chebotar, and S. Levine, “Collective robot reinforcement learning with distributed asynchronous guided policy search,” in *2017 IEEE/RSJ International Conference on Intelligent Robots and Systems (IROS)*. IEEE, 2017, pp. 79–86.
- [11] J. Oh, Y. Guo, S. Singh, and H. Lee, “Self-imitation learning,” in *International Conference on Machine Learning*. PMLR, 2018, pp. 3878–3887.
- [12] T. Hester, M. Vecerik, O. Pietquin, M. Lanctot, T. Schaul, B. Piot, D. Horgan, J. Quan, A. Sendonaris, I. Osband *et al.*, “Deep q-learning from demonstrations,” in *Proceedings of the AAAI conference on artificial intelligence*, vol. 32, no. 1, 2018.
- [13] G. Wang, F. Wu, X. Zhang, J. Liu *et al.*, “Learning diverse policies with soft self-generated guidance,” *International Journal of Intelligent Systems*, vol. 2023, 2023.
- [14] G. Libardi, G. De Fabritiis, and S. Dittert, “Guided exploration with proximal policy optimization using a single demonstration,” in *International Conference on Machine Learning*. PMLR, 2021, pp. 6611–6620.
- [15] Z. Zhu, K. Lin, B. Dai, and J. Zhou, “Self-adaptive imitation learning: learning tasks with delayed rewards from sub-optimal demonstrations,” in *Proceedings of the AAAI Conference on Artificial Intelligence*, vol. 36, no. 8, 2022, pp. 9269–9277.

- [16] A. Gretton, K. Borgwardt, M. Rasch, B. Schölkopf, and A. Smola, “A kernel method for the two-sample-problem,” *Advances in neural information processing systems*, vol. 19, pp. 513–520, 2006.
- [17] A. Gretton, D. Sejdinovic, H. Strathmann, S. Balakrishnan, M. Pontil, K. Fukumizu, and B. K. Sriperumbudur, “Optimal kernel choice for large-scale two-sample tests,” in *Advances in neural information processing systems*. Citeseer, 2012, pp. 1205–1213.
- [18] G. Wang, F. Wu, X. Zhang, and T. Chen, “Policy optimization with smooth guidance rewards learned from sparse-reward demonstrations,” *arXiv preprint arXiv:2401.00162*, 2023.
- [19] J. Schulman, F. Wolski, P. Dhariwal, A. Radford, and O. Klimov, “Proximal policy optimization algorithms,” *arXiv preprint arXiv:1707.06347*, 2017.
- [20] R. S. Sutton, D. A. McAllester, S. P. Singh, Y. Mansour *et al.*, “Policy gradient methods for reinforcement learning with function approximation.” in *NIPS*, vol. 99. Citeseer, 1999, pp. 1057–1063.
- [21] M. Fortunato, M. G. Azar, B. Piot, J. Menick, I. Osband, A. Graves, V. Mnih, R. Munos, D. Hassabis, O. Pietquin *et al.*, “Noisy networks for exploration,” *arXiv preprint arXiv:1706.10295*, 2019.
- [22] Y. Guo, J. Oh, S. Singh, and H. Lee, “Generative adversarial self-imitation learning,” *arXiv preprint arXiv:1812.00950*, 2018.